

Folded Metal and Other Surface Parameters on Combustion Engine Cylinders

Rafael Brisolla Obara^{1,2}, Eduardo Tomanik³, Roberto Martins Souza²
¹Tupy S.A

²Escola Politecnica da Universidade de Sao Paulo

³MAHLE Brazil

Copyright © 2014 SAE International

Abstract

In the last years, sophisticated analyses and control of topography parameters have been introduced to study engine bore cylinders. Such surface characteristics have impact on friction and wear of the engine, with effects on fuel consumption and durability. Among such characteristics, folded metal blocking the honing grooves has received much attention, but its quantification and actual impact on engine performance is still under discussion, both in the academia and in the industry. In this work, a methodology was developed to mathematically quantify the folded metal present in engine bores. The method is compared to others described in the literature and in use by some European automotive manufacturers.

The quantification method, based on topography measurements, was also compared with other analyses, such as optical and scanning electron microscopy. The necessary resolution of the topography measurement and some recommendations for the analysis are given. This work also discusses some limitations of the method, for example, when applied on non-usual bore honing, coated bores or nano-layered bores.

Introduction

The presence of folded metal is characterized by the sealing (partial or total) of the honing grooves in internal combustion engines, which may increase wear and friction on piston rings and eventually cause scuffing (see Figs. 1 and 2). It may also cover graphite veins (Fig. 3) in the engine block and intensify the presence of axial scratches in cylinder bores with detrimental effects on the bore and piston system lubrication, friction and wear. [1, 2, 3].

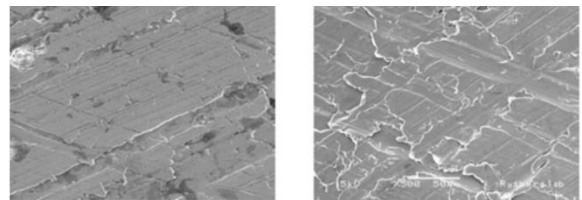


Figure 1. SEM pictures of two cylinder surfaces with different degree of folded material also called "blechmantel" [4].

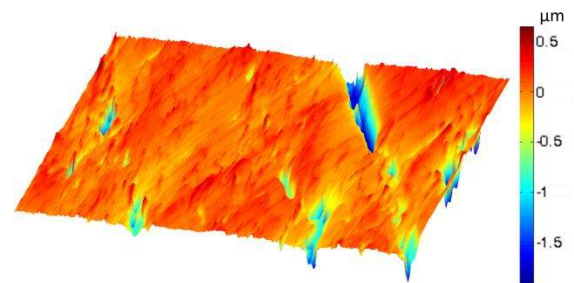


Figure 2. Folded metal covering a honing groove.

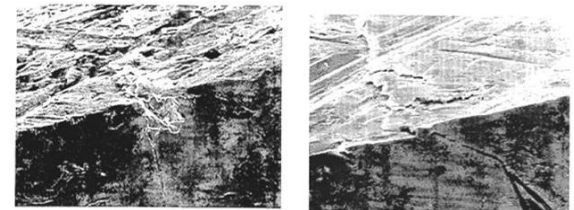


Figure 3. An open graphite vein (at left) and a closed one by folded metal (at right). [1].

Due to the detrimental effects of folded metal, the automotive industry has, for decades, selected visual or destructive methods to quantify folded metal on cylinder liners [1, 5]. With the advance of measurement equipment and computational

numerical analysis, more sophisticated and quantitative methods to characterize cylinder bore topographies have been introduced [6, 7, 8, 9, 10, 11]. Some commercial software incorporate their own routines for quantifying new 3D parameters for honed surfaces, but the lack of standards still hampers the comparison between different methods.

Recently, Mezghani et al. [3] proposed a numerical model to analyze effects of groove interruptions like folded metal on friction between cylinder liner and piston ring. When analyzing a digital surface (simulating an actual honed topography), those authors [3] noticed that the friction coefficient increases by almost 50% when there are discontinuities in the grooves, which may also affect engine behavior and noxious emission.

Profito et al. [12] digitally removed folded metal from actual cylinder liner topographies and analyzed both original and folded metal free topographies in terms of film thickness and friction losses. It was observed that surfaces without folded metal may result in lower friction between cylinder liner and piston ring and may also reduce abrasive wear and vertical scratches.

Surface Measurements and 3D Surface Parameters

3D surface topography measurement has been widely used by academia and industry because of advantages associated with non-contact measurement and high resolution [13]. There are many different 3D parameters used in characterization of honed topographies, such as: Sa, Sk, Spk, Svk, Sds (density of summits of the surface), Ssc (arithmetic mean summit curvature of the surface), Sbi (bearing index), Sci (core fluid retention index) and Svi (valley fluid retention index). Holes, stray grooves, number of grooves, honing angle, distance between grooves, groove interruption, groove width, height and balance and folded metal have also been used in groove characterization [8].

Methods to Quantify Folded Metal

For decades, folded metal was qualitatively compared with amplified images of the surface versus “standards” [5], which are series of reference pictures. However, this method is limited, since it depends on the inspector’s experience.

Gupte et al. [14] suggested using roughness parameters like Ra, Rk, etc. to create a new parameter, “surface index” (SI), which would be related to the folded metal.

Several other researchers have used numerical algorithms to analyze surface topographies. Xin [15] used Radon and Fourier transforms to decompose 3D topographies into two components: one with the grooves and another with the background, as shown in Fig. 4. Dimkovski et al. [6] used a Hough transform to perform similar analysis, but he also quantified folded metal comparing original and ideal images. The percent of folded metal is given by the area that seals the grooves divided by the measurement area. Some commercial software for 3D topography measurement like BMT [16] introduced automatic calculation of folded metal occurrences.

In this work, the folded metal calculation by an in-house code was compared to the ones calculated by the BMT equipment.

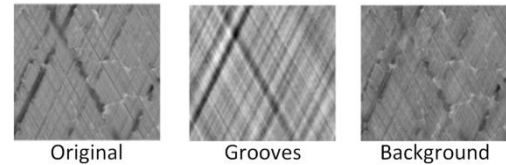


Figure 4. Decomposition of a honed surface image using Radon transform (adapted from [15]).

Although the use of numerical transforms seems to be a promising technique for topography analysis, surface measurement resolution is crucial for an accurate analysis. Fig. 5 shows topographies obtained from two different WLI equipment. Fig. 5 indicates that low quality measurements overlook fine structure elements, which may be confirmed by the lack of high frequency components. For smooth surfaces, high measurement resolution is even more critical due to the difficulty of finding small imperfections in fine honing grooves. Therefore, when small features (as folded metal) are quantified using low resolution equipment, the analysis may not represent the actual condition of the topography.

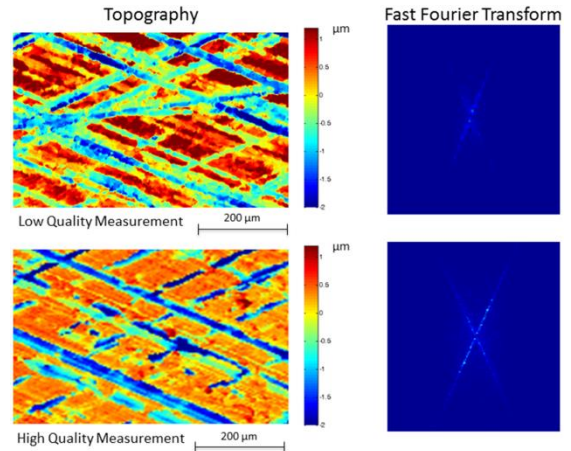


Figure 5. Low and high quality measurements.

For coated bores (Fig. 6) it is possible to create topographies with large pores and without grooves. In this case, folded metal quantification using mathematical transforms will fail because both pores and folded metal are isotropic features. Therefore, it is not possible to locate folded metal regions covering the pores. In order to quantify folded metal in these topographies, a tomography analysis may be required.

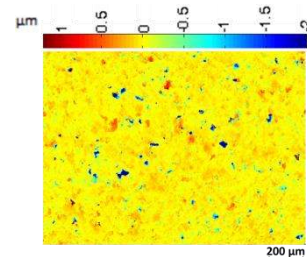


Figure 6. Coated bore topography.

Radon Transform

Mathematically, the Radon transform [17] is obtained by the line integral over a line that is inclined by an angle θ and is located t from the origin. Direct and inverse transforms are given by the following expressions.

$$\mathcal{R}f(t, \theta) =$$

$$\int_{s=-\infty}^{\infty} f(t \cos(\theta) - s \sin(\theta), t \sin(\theta) + s \cos(\theta)) ds \quad (1)$$

$$f(x, y) = \int_0^{2\pi} \mathcal{R}f(\theta, x \cos \theta + y \sin \theta) d\theta \quad (2)$$

The most common application for Radon transform is the tomography, where radiation is used to reconstruct section images of the body. Tissues with different compositions have different levels of radiation absorption. Using specific sensors, it is possible to obtain the integral along the line given by the electron beam, making the image reconstruction possible with high accuracy [18]. In order to reconstruct the original image, infinite projections are needed. Since a finite number of projections is obtained during the tomography, distortions are expected in the reconstructed image.

Besides the medical applications, the Radon transform has also been used in microscopy, astronomy and geophysics [19]. In cylinder liners visual inspection, the Radon transform has been used to separate grooves and background in SEM images [15, 20, 21]. Fig. 7 shows the representation of a honed surface sinogram. Each peak of the sinogram corresponds to a groove on its corresponding honing angle.

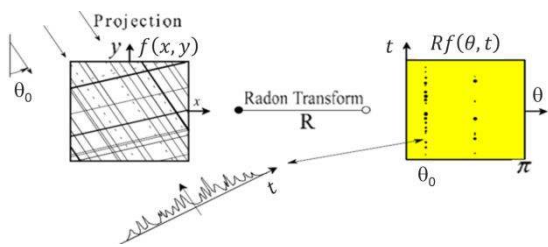


Figure 7. Illustration of the Radon transform (adapted from [20]).

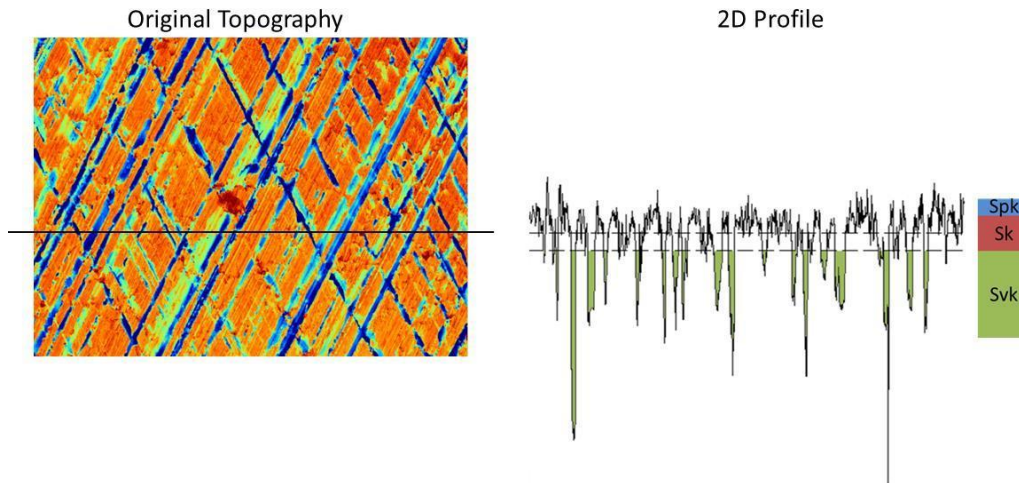


Figure 8. Schematic representation of the honing grooves of the topography.

Quantification of Folded Metal Using the Radon Transform

An algorithm was developed in MATLAB[®] to locate and quantify folded metal using the Radon transform. Initially, the algorithm calculates the topography sinogram, which corresponds to the sum of intensities of pixels over lines inclined by specified angles and located t from the origin (Eq.(1)). Since the topography does not present a rounded shape, the sinogram will contain the sum of more pixels for smaller t values. In order to evaluate grooves near and far from the middle of the topography with same precision, the sinogram is averaged by substituting the sum of intensities of pixels by their average.

The algorithm resets all positions of the averaged sinogram excluding the peaks in the preferential angles (black pixels in the sinogram of the Fig. 9-b), which correspond to values lower than $0.5 \times Sk$ (in relation to the mean plane), and computes the inverse radon transform (Eq. (2)) of the resultant matrix, generating a groove-like image (see Fig. 9-c). In this technique, ascending (Fig. 9-c.1) and descending (Fig. 9-c.2) grooves are analyzed separately.

The groove images are binarized, parallel grooves very close to each other are joined and grooves that do not have at least 30% of their area under the $0.5 \times Sk$ threshold are not considered as grooves (otherwise the algorithm would consider aligned pores as grooves, for example). At the end of these steps, binarized images of ascending and descending grooves are joined (Fig. 9-d).

The occurrence of folded metal is determined by the intersection of the grooves region of the binarized image with pixels of the original topography that are higher than the mean plane. The regions that should be grooves but are not, are considered as folded metal inside the honing grooves. The sum of all those pixels divided by the total number of image pixels provides the percentage of folded metal (Fig. 9-e).

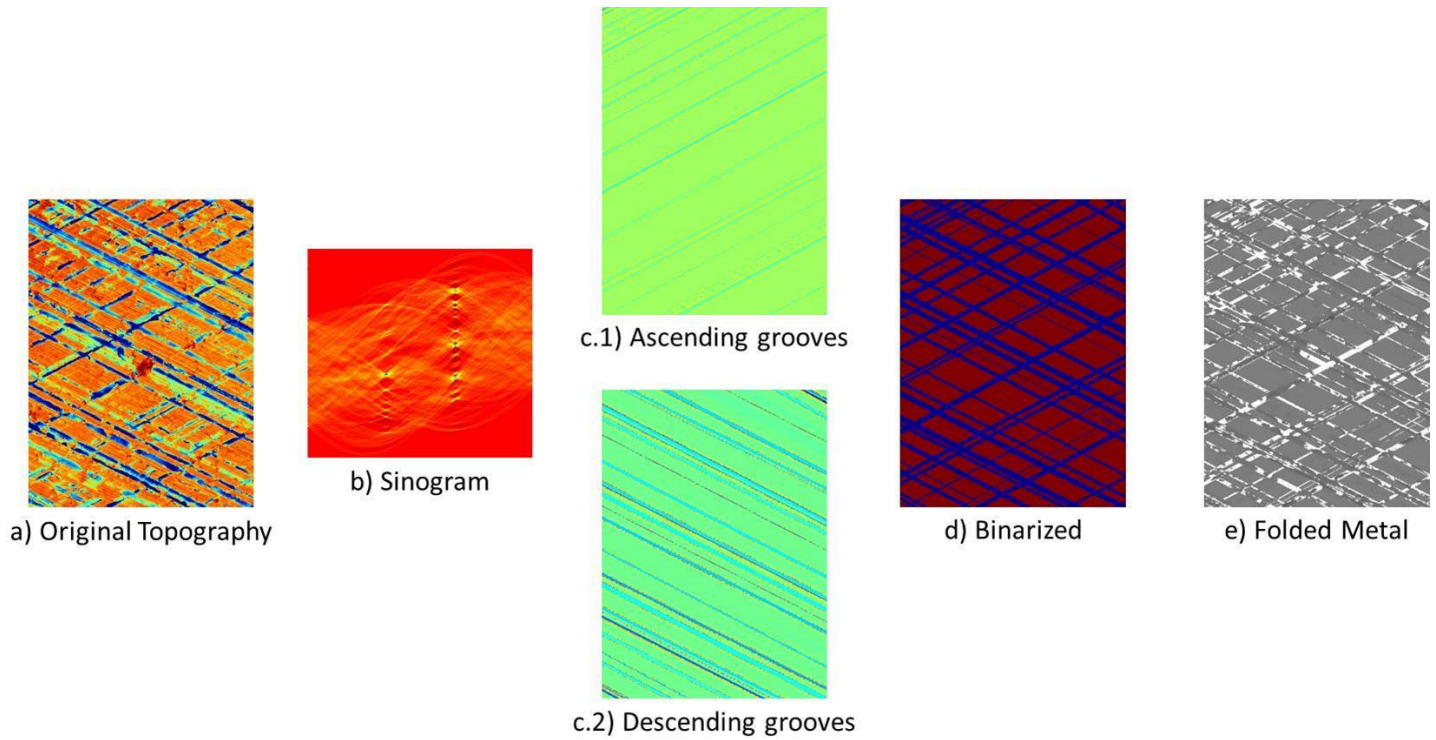


Figure 9. Steps for folded metal quantification using Radon transform.

Correlation of the Developed Method with Commercial Software

This work presents the analysis of two batches with seven heavy duty diesel engine liners in each. One liner batch was honed with diamond honing tools and the other with ceramic tools. The honing parameters were adjusted in order that the two batches had equivalent roughness (S_a , S_k , S_{vk} , S_{pk} ...).

Twelve topographies were obtained for each liner. Aiming the analysis of representative regions, the topographies were obtained for four different angles (0° , 90° , 180° and 270°) and three depths (30 mm, 109 mm and 183 mm).

The 168 topographies were obtained using a BMT white light interferometer (WLI), model WLI Cyl. The equipment is able of analyzing a 1.15×1.56 (mm) region with 1 nm of vertical resolution and $1 \mu\text{m}$ of lateral resolution. BMT equipment also provides a routine for quantifying folded metal; therefore, the topographies were analyzed using both BMT and the proposed method.

The results showed a small positive correlation (see Figures 10 and 11) between the proposed method and the one used in the BMT equipment. In addition, the quantification of folded metal by the proposed method was on average two times higher than the result from BMT software.

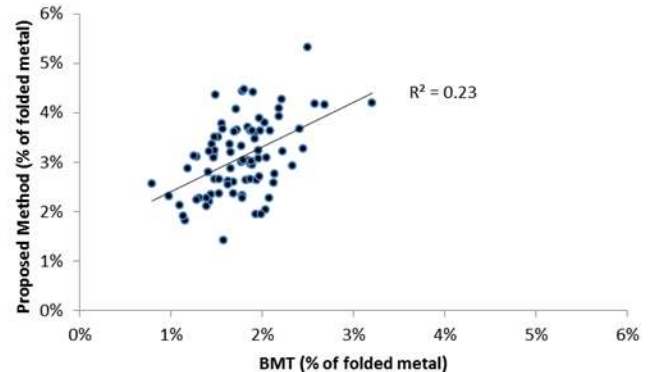


Figure 10. Quantification of folded metal for liners honed with ceramic honing tools.

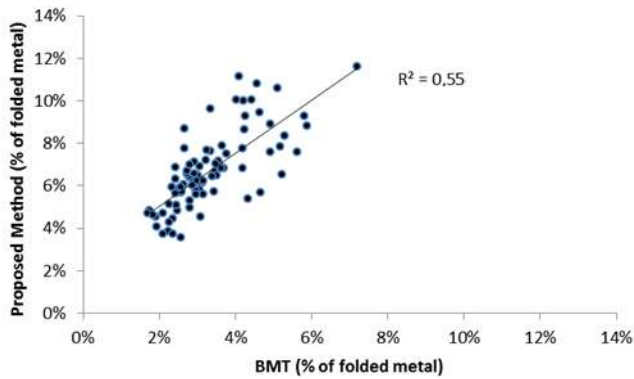


Figure 11. Quantification of folded metal for liners honed with diamond honing tools.

Besides the discrepancies between both methods, a visual analysis of the quantification process allows a better understanding of the reasons that lead to the differences. Fig. 12 shows a comparison between folded metal quantification using BMT software and the proposed method. Fig. 13 shows a zoom of the same topography and, from the visual analysis, the proposed method appears to better identify folded metal occurrences.

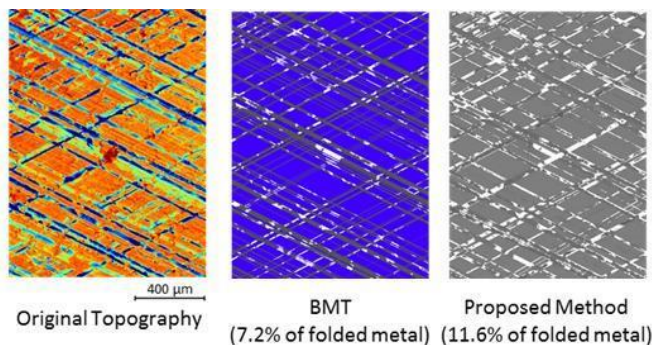


Figure 12. Folded metal occurrence

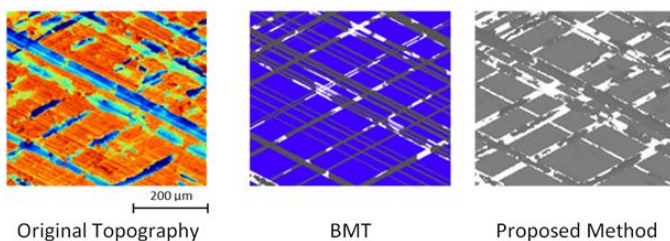


Figure 13. Folded metal occurrence (zoom image).

It was noticed that BMT software considers some large grooves as many small grooves. Furthermore, BMT software also seems to underestimate the width of some grooves (see Fig. 13). Possibly, these are the main reasons that lead the proposed algorithm to locate more regions with folded metal.

Although the diamond honed topography on Fig. 12 had shown that only 11.6% of its area corresponds to folded metal (when analyzing by the proposed method), the folded metal

occurrence was only computed when inside the honing grooves. Since 34.8% of the total area of the honed region corresponds to grooves, it means that folded metal covered one third of the total area of the honing grooves.

Finally, for liners honed with diamond honing tools, the topographies presented in average 6.7% of their total area covered by folded metal (applying the proposed method), which means that folded metal covered 34.9% of the grooves area. For liners honed with ceramic honing tools, the topographies presented in average 3.1% of their area covered by folded metal (applying the proposed method), which means that folded metal covered 25.7%, of the grooves area.

Summary/Conclusions

The implementation of an algorithm for quantifying folded metal using the Radon transform was successfully conducted. Although the proposed algorithm presented significant differences when compared with the BMT software, it seems to better identify folded metal occurrences. The main reasons that lead to the discrepancies between both methods for quantifying folded metal seems to be the underestimation of the width of some honing grooves by the BMT software and the fact that the commercial software also considers some large grooves as many small grooves.

Although the amount of folded metal may seem small when compared with the total area of the topography, folded metal may cover significant portions of honing grooves. For liners honed with diamond and ceramic honing tools, folded metal covered approximately one third and one fourth of grooves area, respectively. Since honing grooves are related with lubricant circulation, folded metal occurrence may significantly increase friction coefficient and abrasive wear.

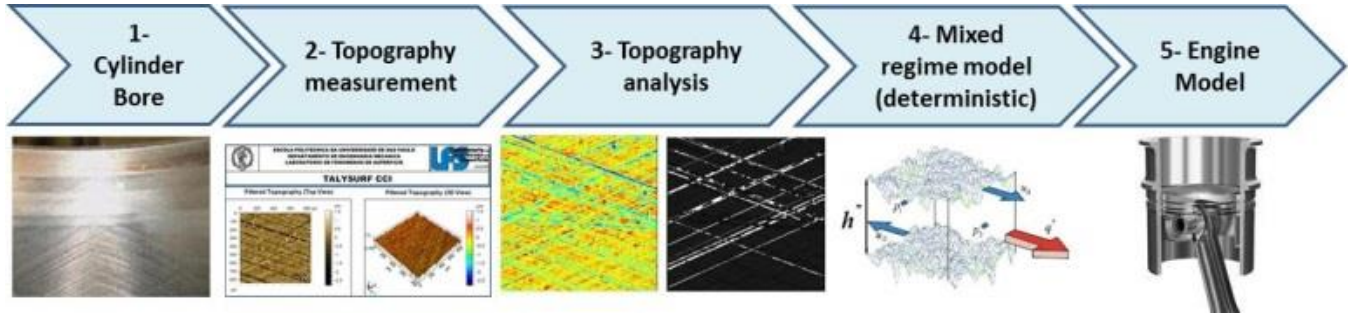
References

1. Tomanik, E., Liner honing quality main characteristics, SAE International (1992) 921453.
2. Papadopoulos, P., Priest, M., Rainforth, W. M., Investigation of fundamental wear mechanisms at the piston ring and cylinder wall interface in internal combustion engines, Proceedings of the IMechE Part J Engineering Tribology 221 (2007) 333–343.
3. Mezghani, S., Demirci, I., Zahouani, H., El Mansori, M., The effect of groove texture patterns on piston-ring pack friction. Precision Engineering. Volume 36, Issue 2, April 2012, Pages 210–217.
4. Anderberg, C., Cabanettes, F., Dimkovski, Z., Ohlsson, R. et al., Cylinder liners and consequences of improved honing. NT2006-11-71. 2006
5. Goetze, Honing Quality handbook.
6. Dimkovski, Z., Anderberg, C., Rosén, B.-G., Ohlsson, R. et al., Quantification of the cold worked material inside the deep honing grooves on cylinder liner surfaces and its effect on wear, Wear 267 (2009) 2235-2242.
7. Sabri, L., Mezghani, S., El Mansori, M., A study on the influence of bond material on honing engine cylinder bores with coated diamond stones. Surface & Coatings Technology 205 (2010) 1515–1519.
8. Dimkovski Z., Anderberg C., Ohlsson R., Rosén B.-G. Complementing 3D roughness parameters for monitoring

- of improved honing of cylinder bores. In Proceedings of the 2nd Swedish Production Symposium, Göteborg, Sweden, November 2008.
9. Pehnelt et al. "Assessment of 3D parameters for the characterization of cylinder treads", MTZ 04/2013
 10. Tomanik, E. Modelling of the Asperity Contact Area on Actual 3D Surfaces. SAE Paper 2005-01-1864, 2005.
 11. Rubach et al. "Wear detection on cylinder liners with optical 3D measuring technology" MTZ 03/2014
 12. Profito, F., Cousseau, T., Tomanik, E., Folded metal effect on lube film thickness and friction using a mixed lubrication deterministic model. SAE International (2014), 2014-06-0302
 13. Stout, K. J., Blunt, L., Three Dimensional Surface Topography. 2nd ed. - London : Penton, 2000.
 14. Gupte, P. S., Wang, Y., Miller, W., Barber, G. C. et al., A Study of Torn and Folded Metal (TFM) on Honed Cylinder Bore Surfaces, Tribology Transactions, Vol. 51, No. 6, p784-789, 2008.
 15. Xin, B., Auswertung und Charakterisierung dreidimensionaler Messdaten technischer Oberflächen mit Riefentexturen. Zur Erlangung des akademischen Grades eines Doktors der Ingenieurwissenschaften von der Fakultät für Maschinenbau der Universität Karlsruhe (TH), 2008.
 16. BMT. WLIInfra, 2014, <http://www.breitmeier.de/en/products/optical-profilometry/wli-infra>
 17. Radon, J., Über die Bestimmung von Funktionen durch ihre integralwerte längs gewisser Mannigfaltigkeiten. Ber. Verch. Sächs. Akad. Wiss. Leipzig Math. Nat. Kd. 69, 262-277, (1917).
 18. Jain, A. K., Fundamentals of Digital Image Processing. New York: PrenticeHall, 1989.
 19. Dhawan, A., Radon Transform. Wiley Encyclopedia of Biomedical Engineering. 2006.
 20. Beyerer, J., Leon, F. P., Detection of defects in groove textures of honed surfaces, International Journal of Machine Tools and Manufacture 37(3): 371–389. 1997.
 21. Leon, F. P., Evaluation of Honed Cylinder Bores. CIRP General Assembly, San Sebastián, Spain, 18–24 August 2002, CIRP Annals, Vol. 51/1, 2002.

Appendix

The developed code and this paper is part of the LFS (Laboratory of Surface Phenomena) of the Escola Politecnica - USP approach for engine cylinder tribological optimization that aims to reduce friction losses, hence fuel consumption etc. The work is being carried inside the R&D consortium "TriboFlex", Desafios Tribológicos para Futuras Gerações de Motores Flex-Fuel, FAPESP PIT project number 2009/54891-8.



All rights reserved. No part of this publication may be reproduced, stored in a retrieval system, or transmitted, in any form or by any means, electronic, mechanical, photocopying, recording, or otherwise, without the prior written permission of SAE.

ISSN 0148-7191

©Copyright 2014SAE International.

Positions and opinions advanced in this paper are those of the author(s) and not necessarily those of SAE. The authors solely responsible for the content of the paper.